Design of feedback controllers for paraplegic standing

K.J.Hunt, H.Gollee, R.-P.Jaime and N. de N.Donaldson

Abstract: The development, implementation and experimental evaluation of feedback systems for the control of the upright posture of paraplegic persons in standing is described. While the subject stands in a special apparatus, stabilising torque at the ankle joint is generated by electrical stimulation of the paralysed calf muscles of both legs using surface electrodes. This allows the subject to stand without the need to hold on to external supports for stability— this is termed 'unsupported standing'. Sensors in the apparatus allow independent measurement of left and right ankle moments together with measurement of the inclination angle. A nested loop structure for control of standing is implemented, where a high-bandwidth inner loop provides control of the ankle moments, while the angle controller in the outer loop regulates the inclination angle. A number of important modifications to a control strategy which was previously tested with both neurologically intact and paraplegic subjects are presented. The new strategy is described, and an experimental evaluation with intact subjects is reported. The experimental results show that the control system for unsupported standing performs reliably, and according to the design formulation. There are a number of design choices, appropriate to different situations, and the practical effect of each is clear. This allows easy 'tuning' during an experimental session. This is important since the complete design procedure, from muscle dynamics identification to control design, has to be carried out as quickly as possible while the subject is standing in the apparatus. A number of recommendations are made regarding the preferred design choices for control of unsupported standing.

1 Introduction

This paper describes the development, implementation, and experimental evaluation of feedback systems for the control of the upright posture of paraplegic persons in standing. While the subject stands in a special apparatus, stabilising torque at the ankle joint is generated by electrical stimulation of the paralysed calf muscles of both legs. This allows the subject to stand without the need to hold on to external supports for stability—we call this 'unsupported standing'.

Spinal cord injury results in an interruption of the neurological pathway from the brain to the muscles. A complete lesion of the spinal cord in the back (at thoracic level) results in paralysis of the lower limbs, and the loss of voluntary control of the muscles below the level of the lesion. Paralysed muscles do, however, generally retain their ability to contract, and electrical stimulation can be used in rehabilitation as a therapy. Stimulation restores muscle bulk and can bring several other benefits [1]. With functional electrical stimulation (FES), the aim is to restore some normal motor activities to the muscles [2]. Such activities include standing up [3, 4], standing [5, 6], stepping [7], and cycling [8, 9].

We have been developing feedback systems for control of unsupported standing in complete paraplegia [5, 10–12]. In its simplest form, the body is regarded as a single-link inverted pendulum with movement only around the ankle joint. Experimentally, this situation has been realised by standing subjects in an apparatus known as the 'Wobbler' [13], as shown in Fig. 1. While standing in the apparatus, the subject is strapped into a custom-made body brace which locks the knee and hip joints. The stabilising ankle moment which is required to maintain upright posture is generated by stimulation of the calf muscles. In our experiments surface electrodes have been used. Electrode placement on the calf muscles is shown in Fig. 2.

Sensors in the Wobbler apparatus allow independent measurement of left and right ankle moments, together with measurement of the inclination angle. This has allowed us to implement a nested loop structure for control of standing (see Fig. 3): a high-bandwidth inner loop provides control of the ankle moments via stimulation of the calf muscles; the angle controller in the outer loop regulates the inclination angle, and its control signal is the desired ankle moment for the inner loop.

In previous work [5], we designed LQG controllers for both moment control and angle control. These controllers were tested with both neurologically intact and paraplegic subjects [6]. We found that the intact subjects could stand using these controllers for long periods of time. With paraplegic subjects, however, only short periods of stable standing were possible (typically 15–20 s). In order to

IEE Proceedings online no. 20010254

DOI: 10.1049/ip-cta:20010254

Paper first received 15th December 1999

K.J. Hunt, H. Gollee and R.-P. Jaime are with the Centre for Systems and Control, Department of Mechanical Engineering, University of Glasgow, Glasgow G12 8QQ, UK

N. de N. Donaldson is with the Department of Medical Physics and Bioengineering, University College London, London WC1E 6JA, UK

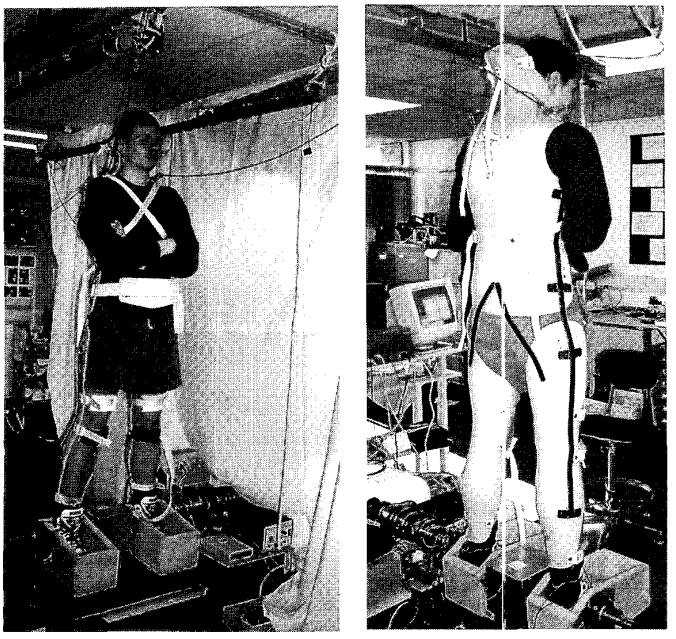

Fig. 1 *Two views of subject standing in Wobbler apparatus*

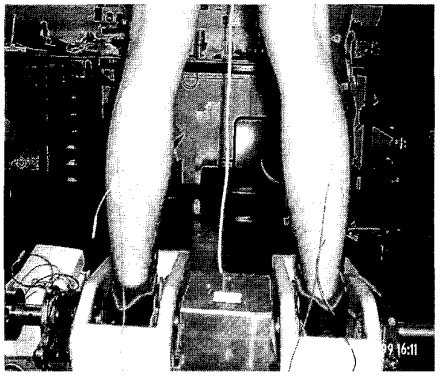

Fig. 2 *Placement of electrodes on calf muscles (body brace removed to reveal electrode positions)*

improve the reliability and consistency of the control system, and to achieve longer periods of unsupported

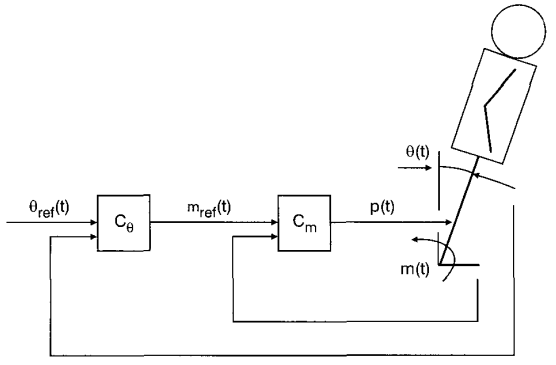

Fig. 3 *Nested loop control structure. θ is inclination angle, m is ankle moment, and p is pulsewidth of stimulation. C_m is moment controller and C_θ is angle controller. Desired values for ankle moment and inclination angle are m_{ref} and θ_{ref}, respectively*

standing with paraplegic subjects, we have made several important changes to the control design approach. Our new strategy is described in this paper, and experimental evaluation with intact subjects is reported.

The key design changes which have been implemented are:

- Pole assignment (PA) design is used instead of LQG. The desired closed-loop poles (control poles and observer poles) are selected indirectly using the corresponding risetime and damping of equivalent linear second-order transfer functions. This has the advantage that the nominal closed-loop response is independent of the nominal plant model (not so with LQG). This is important because the dynamics of the electrically stimulated muscle can vary significantly between individuals.
- The moment control loop is now treated as a SISO system. The same stimulation pulsewidth is applied to left and right legs, and the measured output is now the total ankle moment. Previously, separate controllers were designed for left and right moments, and the legs were individually stimulated. The total desired moment was split equally between both sides. The new approach has the advantage that total moment is balanced between both legs in a natural way, depending on the ability of each leg to deliver force for a given stimulation level. This is important because paraplegic subjects often have a strongly asymmetric left/right response, and therefore it is not reasonable to demand the same moment from both sides. However, it remains to be seen in paraplegic experiments whether this strategy results in significant movement out of the sagittal plane.
- The moment control loop is now usually designed without integral action, which means that higher bandwidths can be achieved in this loop.
- The closed-loop characteristics of the inner loop can now be treated as part of the plant for the outer loop (angle loop) design. It is shown that this allows achievement of stability even when the inner loop is relatively slow. Previously, the inner loop was neglected under the assumption that it has a relatively high bandwidth. Often,

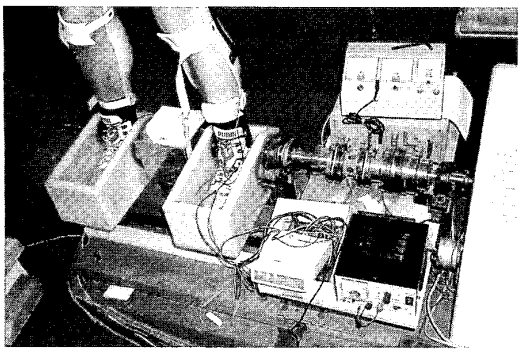

Fig. 4 *Position of feet in footboxes and moment measuring load cells*

however, the inner loop can become slow (due, for example, to fatigue or low muscle power) resulting in system instability.

- A new notch filter design approach for the outer loop is implemented, for the case where the inner loop is included in the design. The inner loop is relatively fast compared to the outer loop, and having a notch design can avoid certain problems of numerical and measurement noise sensitivity in the design.

These various design options give considerable flexibility, and the effect of the design choices is experimentally evaluated. Our goal has been to develop an approach having a set of design parameters with a clear physical interpretation. This is important because experimental use of the control system in the rehabilitation laboratory involves people who do not necessarily have expertise in control engineering (e.g., bioengineers, clinicians and physiotherapists). This is also important because system identification and control design must be done during experimental sessions *while the subject is standing in the apparatus*—the design procedure must therefore be carried out quickly.

2 Methods

2.1 Apparatus

The Wobbler apparatus is described in detail in [13]. The Wobbler has been designed to allow investigation of artificial control strategies for unsupported standing without interference from the brain. To this end, a custom-fitted body shell is worn, which locks the knee and hip joints; the subject is therefore free to rotate only around the ankle joint. The feet are positioned in footboxes as shown in Fig. 4. A load cell between the two boxes allows measurement of the moment in the right ankle. A load cell to the left of the footboxes measures total ankle moment. A string attached to the body brace at shoulder level is wound round a pulley attached to a potentiometer placed well behind the subject. This potentiometer is used to measure the inclination angle. Four light ropes are attached to the shoulders of the body brace, and from there to a frame attached to the ceiling. These ropes are for safety and prevent the subject falling backwards or forwards too far. During muscle identification and ankle moment control tests the four ropes are kept taut. For angle control experiments the ropes are slackened sufficiently to allow movement back and forth within pre-defined limits.

For stimulation of the muscles we use the 'Stanmore Stimulator' as described in [14], connected to electrodes which are placed on the skin over the calf muscles as shown in Fig. 2. The stimulator provides current controlled monophasic rectangular pulses up to a pulse duration of 500 μs. In these experiments the stimulator operates at a constant frequency of 20 Hz (sample interval 50 ms). At the start of each experiment the current is set at a desired constant level (see test C described below). Thus, during the experiments the stimulation pulses have constant frequency and amplitude, and the pulsewidth is varied.

The stimulator is driven via a serial line from a PC. The signals from the load cells and angle-measuring potentiometer are connected to the PC via an analogue–digital conversion card. For control purposes the moments and angle are sampled at 20 Hz (sample time 50 ms), which is the same as the stimulator frequency. Real-time data acquisition and control on the PC is implemented within Matlab/Simulink running the Real-time Toolbox [Note 1].

A schematic diagram of the arrangement of sensors and stimulation equipment for the ankle moment control loop is shown in Fig. 5.

2.2 Tests

During each experimental session the subject is first secured in the apparatus, and then a set of five principal tests is carried out:

(*i*) Test C: The purpose of this test is to establish a suitable stimulation current level for the experiment. Starting with a low current, the pulsewidth is ramped up in steps of 2 μs from 0 to 500 μs and the moment is measured. The current is then incremented by 10 mA and the stimulation pattern is repeated. This process continues until the muscle is seen to be saturating at high pulsewidths, while ensuring the subject is still comfortable. The current is fixed at this level for the remainder of the experiment. This procedure is carried out for each leg separately.

(*ii*) Test PRBS: This is an open-loop test using a stimulation signal where the pulsewidth has a PRBS [Note 2] form. The same stimulation pulsewidth is applied to both legs and the total moment (left + right moments) is measured. The PRBS signal can be applied around a range of mean stimulation pulsewidth levels. The amplitude of the PRBS signal at each mean level was set at 35 μs. The PRBS signal which we used has a period of 155 samples and is constant for at least five samples after each transition [15].

The input/output data arising from the PRBS tests are used to identify local linear transfer functions at each operating point. One of the models is chosen as the nominal model for moment control design. Moment control design is then carried out as described in Section 3. Following design and analysis of the controller, a closed-loop moment control test is carried out:

(*iii*) Test M: This is a test of closed-loop moment tracking. Typically, a square-wave reference moment of a given amplitude and frequency is applied.

Following analysis of the total moment control system, the design parameters are sometimes changed and test M repeated. This process is continued until satisfactory results are obtained (usually only one or two iterations are required). The design parameters for the angle control loop are then selected, the angle controller is designed, and two kinds of closed-loop angle control tests are carried out.

(*iv*) Test T: This is a test of closed-loop angle tracking. Typically, a square-wave reference angle of a given amplitude and frequency is applied. Sometimes, in a procedure

Note 1: Humusoft s.r.o. (http://www.humusoft.com)
Note 2: Pseudo-random binary sequence

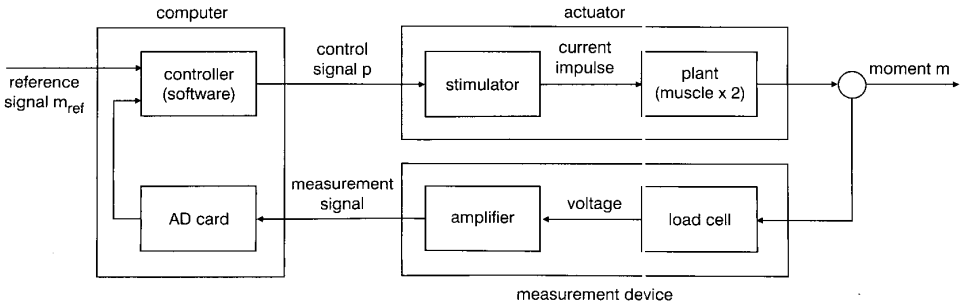

Fig. 5 *Arrangement of ankle moment sensor and stimulator*

known as 'quiet standing', the reference angle is kept constant.

(*v*) Test D: This is a test of closed-loop disturbance rejection. Here, the reference angle is kept constant and disturbances are applied to the body. We applied disturbances by repeatedly pulling the subject forwards or pushing him back.

2.3 Subjects

All experiments reported here were carried out with neurologically intact and fit male subjects. It is important to work initially with intact subjects in order to evaluate and verify the control approach and the hardware and software configuration. Working with intact subjects naturally raises the question of whether voluntary postural control inputs can affect the observed results, but the experiments have been designed to ensure that such effects are minimised. During an experiment the subject stands quietly with arms folded across the chest and eyes closed. Thus the subject receives no cognitive feedback regarding the moment and angle setpoints, or of the current inclination angle. The subject also loses proprioception from the ankles and exteroception from the soles of the feet. Indeed, most intact subjects report that the electrical stimulation of the calf muscles causes a loss of normal sensation in their lower limbs, and that they found it easy to 'submit' themselves to the artificial control system. In these circumstances it is clearly impossible for subjects to voluntarily achieve accurate tracking of the inclination angle setpoint.

3 Design approach

The nested-loop structure for unsupported standing (see Fig. 6) allows the overall feedback control system to be designed and tested in several steps, starting with the ankle moment control loop and moving then to the body angle controller. The steps involved in system design and test are:

(*i*) The muscle dynamics are identified using the open-loop PRBS test. This establishes a dynamic model between the pulsewidth p and the ankle moment m. This step also involves validation of the identified models.

(*ii*) The closed-loop controller for ankle moment is designed; this step establishes a desired closed-loop response between the reference moment m_{ref} and the measured moment m. Following controller synthesis, the moment loop is verified by examining the key closed-loop frequency responses, and then by testing the realtime performance (test M). When these tests are judged to be satisfactory we proceed to the next step.

(*iii*) The closed-loop controller for body inclination angle is designed. The plant for angle controller design is taken as the transfer function between the desired moment m_{ref} and the angle θ, i.e., this is a combination of the ankle moment loop and the open-loop body dynamics (see Section 3.3 for further details of this approach). Angle controller design establishes a desired closed-loop response between the reference angle θ_{ref} and the measured angle θ. The frequency response functions of the overall closed loop are verified, and then the system is tested in realtime (with tests T and D).

Details of the approach used for muscle dynamics identification are given elsewhere [12, 16], but it should be noted that here the same stimulation pulsewidth is applied to both legs, and the output is taken as the total ankle moment (previously, left and right sides were identified and controlled separately). Thus, the physical realisation of the block labelled 'muscle' in Fig. 6 is as shown in Fig. 7.

The underlying design approach for both of the control loops is pole assignment; the generic design approach is described in Section 3.1. Specialisation of the generic approach for the ankle moment loop is presented in Section 3.2, and for the angle controller in Section 3.3.

3.1 Generic design approach

The generic feedback control structure is shown in Fig. 8. The open-loop plant is represented by the discrete-time model

$$y(t) = \frac{q^{-k}B(q^{-1})}{A(q^{-1})}u(t) + \frac{1}{\Delta(q^{-1})A(q^{-1})}d(t) \qquad (1)$$

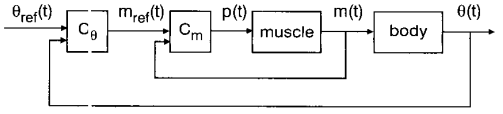

Fig. 6 *Nested loop structure for unsupported standing*

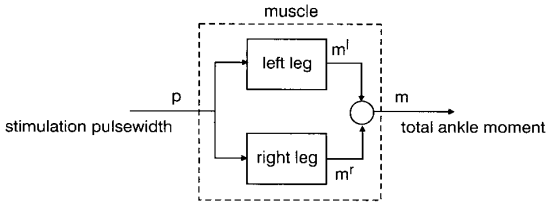

Fig. 7 *Arrangement of left and right stimulation signals. Common stimulation pulsewidth p is applied to both sides, resulting in left and right moments m^r and m^l. Total moment is then $m = m^l + m^r$. Muscle identification estimates dynamic response from pulsewidth p to total moment m. Ankle moment controller is SISO system with reference which is total desired moment m_{ref} and controlled output of total moment m*

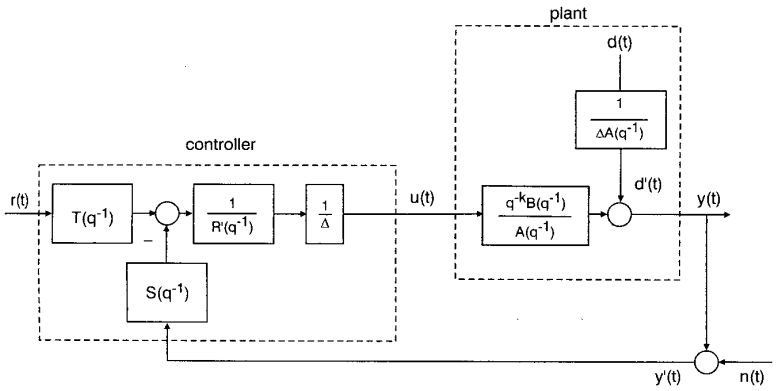

Fig. 8 *Generic feedback control loop structure. Note that* $A(q^{-1})R'(q^{-1}) = R(q^{-1})$

Here, $y(t)$ is the plant output, $u(t)$ is the input, and $d(t)$ is a disturbance term. The integer $k \geq 1$ is a discrete input–output time delay, while A and B are polynomials in the delay operator q^{-1} defined by

$$A(q^{-1}) = 1 + a_1 q^{-1} + \cdots + a_{na} q^{-na} \tag{2}$$

$$B(q^{-1}) = 1 + b_0 q^{-1} + \cdots + b_{nb} q^{-nb} \tag{3}$$

The net effect of disturbances is represented at the output by the signal d driving the filter

$$\frac{1}{\Delta(q^{-1})A(q^{-1})}.$$

The polynomial Δ will be defined, depending on the context, as either $\Delta = 1$ or $\Delta = 1 - q^{-1}$. In the latter case, the output disturbance models the effect of stepwise-changing (piecewise constant) disturbances and offsets, which typically result from physiological and environmental factors [Note 3]. The choice of Δ directly determines whether or not integral action should be included in the controller (see below).

The plant output $y(t)$ is assumed to be corrupted by measurement noise $n(t)$ so that the signal

$$y'(t) = y(t) + n(t) \tag{4}$$

is available for feedback. The control signal $u(t)$ in Fig. 8 is defined by

$$u(t) = \frac{1}{R(q^{-1})}(T(q^{-1})r(t) - S(q^{-1})y'(t)) \tag{5}$$

with $r(t)$ a reference signal. The controller polynomials R, S and T are to be determined in the design procedure. Note that R is constrained to have Δ as a factor, i.e. $R = \Delta R'$ (see Fig. 8).

The closed-loop equation resulting from eqns. 1 and 5 is

$$y(t) = \frac{q^{-k}B(q^{-1})T(q^{-1})}{\rho(q^{-1})}r(t) + \frac{R(q^{-1})}{\Delta(q^{-1})\rho(q^{-1})}d(t) - \frac{q^{-k}B(q^{-1})S(q^{-1})}{\rho(q^{-1})}n(t) \tag{6}$$

Here the closed loop characteristic polynomial is denoted as ρ, and is given by $\rho = AR + q^{-k}BS$. For the purposes of later analysis, the sensitivity function $\tilde{S}$ (the transfer function from disturbance term $d' = d/\Delta A$ to output y) and the complementary sensitivity function $\tilde{T}$ (the transfer function from measurement noise n to output y) are seen to be

$$\tilde{S} = \frac{A(q^{-1})R(q^{-1})}{\rho(q^{-1})}, \quad \tilde{T} = \frac{q^{-k}B(q^{-1})S(q^{-1})}{\rho(q^{-1})} \tag{7}$$

In a standard pole assignment design the desired closed-loop characteristic polynomial is split into two parts, one denoted as A_m, which is primarily used to specify the desired poles of the command tracking response, and the other denoted as A_o, known as the *observer polynomial*, which has further influence on the properties of the feedback loop [18]. Thus, in the standard formulation of pole assignment, the equation $AR + q^{-k}BS = A_m A_o$ is solved for R and S. A further possibility, however, is to allow for cancellation of fast or oscillatory plant poles. This is known as a *notch filter* design since these modes will not then be excited. The plant denominator is factored as $A = A^+A^-$, where A^+ includes the poles to be cancelled by the controller. Any plant poles which are cancelled will become poles of the closed-loop system, and the closed-loop characteristic equation therefore becomes

$$\rho = A^+A^-R + q^{-k}BS = A_m A_o A^+ \tag{8}$$

For solvability of this expression the polynomial S must also contain A^+ as a factor. Writing $S = A^+S'$, the design equation

$$A^-R + q^{-k}BS' = A_m A_o \tag{9}$$

is obtained. The structure of R is determined by the choice of the polynomial Δ in the noise model. When $\Delta = 1 - q^{-1}$, i.e., stepwise changing constant disturbances are present, then integral action must be included in the controller to achieve zero steady-state tracking error, which amounts to constraining R as $R = \Delta R'$. Substituting in eqn. 9, the final design equation becomes

$$A^-\Delta R' + q^{-k}BS' = A_m A_o \tag{10}$$

The design equation is solved for R' and S' subject to the condition

$$(A^-\Delta)^{-1}S' \quad \text{strictly proper} \tag{11}$$

i.e., $\deg(S') < \deg(A^-) + \deg(\Delta)$. A sufficient condition to ensure the existence of a unique solution with this property is that the polynomials A^- and B have no common factors [19].

Note 3: In a stochastic framework, d is often taken as a compound or generalised Poisson process. See [17] for details.

Finally, the polynomial T is designed to achieve suitable command tracking. From eqn. 6 the transfer function $G_{y/r}$ from r to y is given by

$$G_{y/r} = \frac{q^{-k}B(q^{-1})T(q^{-1})}{\rho(q^{-1})} = \frac{q^{-k}B(q^{-1})T(q^{-1})}{A_m(q^{-1})A_o(q^{-1})A^+(q^{-1})} \quad (12)$$

In order to avoid excitation by the reference signal of system modes contained in the observer polynomial A_o, or the possibly fast or oscillatory modes in A^+ these two factors are cancelled by appropriate definition of T. T must also ensure unity steady-state gain in $G_{y/r}$, and is therefore defined as

$$T(q^{-1}) = \lambda A_o(q^{-1})A^+(q^{-1}) \quad (13)$$

where the scalar λ is

$$\lambda = \frac{A_m(1)}{B(1)}.$$

This results in

$$G_{y/r} = \frac{q^{-k}B(q^{-1})A_m(1)}{A_m(q^{-1})B(1)} \quad (14)$$

as desired. (It is assumed that $B(1) \neq 0$.) Note that by placing further constraints on the controller polynomials stable factors of the plant B polynomial could also be cancelled, but this was not required in the experiments reported here.

It is clear from eqn. 14 that the closed-loop tracking properties are determined by choice of A_m. However, A_m does also have a direct influence on the disturbance rejection and measurement noise properties of the feedback system (see eqn. 6). It is possible to decouple command tracking from the internal properties of the closed-loop by defining a reference pre-filter, which cancels the stable poles in A_m and replaces them by an alternative set of tracking poles. However, this was not utilised here since satisfactory overall performance was achieved without this option.

The polynomials A_m and A_o are chosen here using a time-domain approach to correspond to the poles of second order transfer functions having a specified risetime and damping. For the control poles A_m these design variables are denoted as t_m^r and ζ_m. For the observer poles they are written t_o^r and ζ_o (See [12] for further details of this method.)

The design approach outlined above can be summarised in the following design steps:

Given data: A, B, k
Choose design parameters: Δ, t_m^r, ζ_m, t_o^r and ζ_o
Choose design parameter: A^+ by factorising A and writing $A = A^+A^-$, with A^+ chosen as the factors of A which are to be cancelled

Step 1: Compute A_m and A_o (from t_m^r, ζ_m and t_o^r, ζ_o)
Step 2: Solve the design equation

$$A^-\Delta R' + q^{-k}BS' = A_mA_o$$

for R' and S' subject to the condition $\deg(S') < \deg(A^-) + \deg(\Delta)$
Step 3: Form the polynomials S and R using

$$S = S'A^+, \quad R = R'\Delta$$

Step 4: Form the polynomial T using

$$T = \lambda A_oA^+$$

with $\lambda = A_m(1)/B(1)$
After this design procedure has been carried out the sensitivity functions in eqn. 7 are normally checked and the closed-loop performance is evaluated. If necessary, the design parameters can be changed and the procedure repeated. The experimental results show the effects of varying some of the design parameters.

3.2 Ankle moment control

The generic design approach is straightforwardly specialised for ankle moment control by the following definitions: the controlled output y is in this case total moment m, the control signal u is the stimulation pulsewidth p, and the reference r is the desired total moment m_{ref}. The plant polynomials A and B (together with the integer k) are obtained from the identification experiments. With a sample time of 50 ms we found that the best value for k was $k = 1$. Typically, the muscle dynamics are stable and second order [16]. Experimental results are shown below for moment control with and without integral action (i.e., for $\Delta = 1 - q^{-1}$ and $\Delta = 1$, respectively). The notch filter design option is never used for moment control, i.e., $A^+ = 1$.

3.3 Body angle control

To use the generic procedure for designing inclination angle controllers the following definitions are made: the controlled output y is the angle θ, the control signal u is the desired moment m_{ref} for the inner loop, and the reference r is the desired angle θ_{ref}.

The body dynamics are approximated using the simple model shown in Fig. 9. Due to the rigid body brace worn by the subject the system can be viewed as a single-link inverted pendulum. The equation of motion of the rigid body dynamics, free only to move about the ankle, and maintained upright by a variable moment m about the ankle is

$$-m + \tilde{m}gl\sin\theta = J\frac{d^2\theta}{dt^2} \quad (15)$$

In this equation $\tilde{m}$ is the mass and J is the moment of inertia. The centre of gravity is assumed to be at length l from the ankle joint and g is gravitational acceleration. For small inclination angles we have $\sin\theta \approx \theta$, and the linearised transfer function of the body dynamics becomes

$$\frac{\Theta(s)}{M(s)} = \frac{-1/J}{s^2 - \tilde{m}gl/J} \quad (16)$$

where s is the Laplace transform complex variable and capitals indicate transformed signals. The biomechanical parameters $\tilde{m}$, l and J can be measured for each subject using a simple procedure outlined in [5].

There are two options which have been followed for determination of the plant for angle controller design (this plant is the transfer function from m_{ref} to θ):

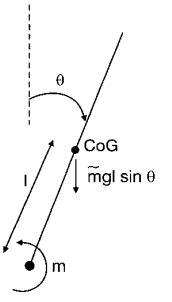

Fig. 9 *Biomechanical system*
CoG is centre of gravity

(i) The first option is to neglect the dynamics of the ankle moment loop, and base the design only on the biomechanical model. The justification for investigating this route is that the inner loop is of relatively high bandwidth. In this case the design plant B/A is obtained simply by discretising the dynamics in eqn. 16.
(ii) The second option is to include the inner-loop dynamics in the design plant. In this case the plant B/A is obtained by cascading the discretised body dynamics eqn. 16 with the known closed-loop transfer function of the inner loop (i.e., using 14 from inner loop design). This procedure assumes that the sample rates for both loops are the same, which is the case in the experiments reported here. Alternatively, a multirate sampling approach, as described in [5], can be adopted.

Experimental results for both cases are reported in the sequel.

The angle controller is always designed to have integral action ($\Delta = 1 - q^{-1}$). When the moment loop is included in the angle controller design plant (option (ii) above), then usually a notch filter is implemented for angle controller design (experimental results are described below for tests with and without notch design). When used, the purpose of the notch filter is to cancel the (relatively fast) dynamics of the moment loop. In this case we select $A^+ = A_m^{moment}$, where A_m^{moment} signifies the closed-loop design polynomial A_m used for the moment loop, and $A^- = A^{body}$, where A^{body} signifies the denominator of the discretised body dynamics eqn. 16.

4 Experimental results

In this Section we present the results of experimental evaluation of feedback controllers for unsupported standing, following the experimental protocol outlined in Section 2.2. The aim was to investigate the effect of the available design choices, in particular:

- Design of ankle moment controllers with and without integral action (Section 4.3).
- The effect of the speed (bandwidth) of the moment control loop on the stability of the overall system (Section 4.4).
- The effect of, and potential improvements resulting from, inclusion of the inner loop dynamics in the plant used for angle loop design (Section 4.4).
- The effect and need for the notch filter design approach for angle control design (Section 4.4).

First, typical results from test C (current selection) and test PRBS (for muscle dynamics identification) are presented (Sections 4.1 and 4.2).

A short video sequence corresponding to the results of the tests T and D can be viewed in [20].

4.1 Setting the current level

Typical results of test C are shown in Fig. 10. This shows that for a current of 40 mA the muscle is response is very weak, whereas when stimulated with a current of 60 mA the muscle output saturates for relatively small pulsewidths. Choosing a stimulation current of 50 mA enabled us to use the full range of the pulsewidth, and this value was fixed for the remainder of the experiment.

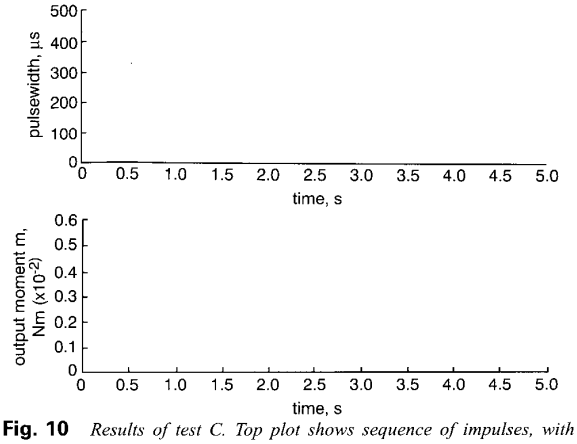

Fig. 10 *Results of test C. Top plot shows sequence of impulses, with ramping pulsewidth, applied to muscle. Bottom plot shows measured moment for three different current levels: 40, 50 and 60 mA*

—— 40
– – – 50
· · · · 60

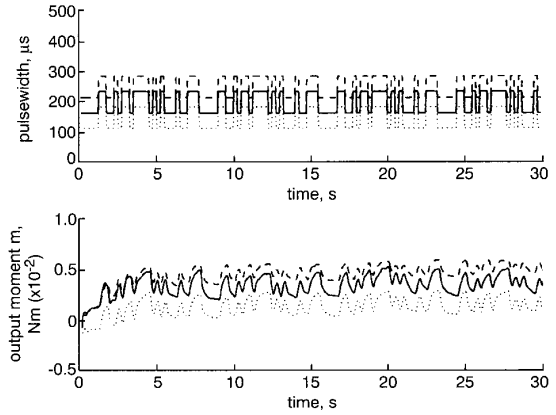

Fig. 11 *Muscle identification data for various mean levels of PRB input signal (amplitude 35 μs). The top curves show PRBS input signals (pulsewidths) while the bottom curves show the measured moments corresponding to each level of input*

· · · · 150 μs
– – – 250 μs
—— 200 μs

4.2 Muscle identification tests

Results of test PRBS are shown in Fig. 11. The dynamic models identified for the three levels of input-output data are shown in Table 1. For the design of the muscle moment controllers, we choose to work with the model with the highest gain to ensure robust stability of the moment loop for varying stimulation levels, i.e., the model identified for a mean pulsewidth of 200 μs.

Table 1: Identification results for linear muscle models. Sample time is 50 ms

Mean pw, μs	$G(q^{-1})$	Gain ($\times 10^{-3}$)	Poles
150	$(4.3 \times 10^{-4} q^{-1})/(1 - 1.30q^{-1} + 0.44q^{-2})$	3.05	$0.65 \pm 0.13i$
200	$(4.0 \times 10^{-4} q^{-1})/(1 - 1.32q^{-1} + 0.43q^{-2})$	3.55	0.70; 0.62
250	$(2.8 \times 10^{-4} q^{-1})/(1 - 1.35q^{-1} + 0.45q^{-2})$	2.71	0.74; 0.61

4.3 Ankle moment control tests

Results of closed-loop moment tracking, test M, are shown in Figs. 12 and 13. Fig. 12 shows a design where integral action is included in the controller, i.e. $\Delta = 1 - q^{-1}$ (see eqn. 10), whereas no integral action ($\Delta = 1$) was used for the results presented in Fig. 13. The sensitivity functions for the controllers used in the results of Figs. 12 and 13 are shown in Figs. 14 and 15, respectively.

4.4 Body angle control tests

The results reported here are for a subject with physical parameters $J = 90$ N ms^2, $\tilde{m} = 90$ kg and $l = 1$ m (see eqns. 15 and 16). Results of the closed loop angle tracking and disturbance rejection tests, test T and test D, are shown. (See also [20] for a short video sequence showing a similar experiment.) Here, a square wave with a period of 20 s is used as the reference. For the first 20 s, no external disturbances are explicitly applied, which corresponds to 'quiet standing', test T. During the remaining 20 s, the standing is disturbed by pulling the subject forward (at $t = 25$ s) and by pushing him backwards ($t = 35$ s).

A combination of different design choices are shown, c.f. Section 3.3. The design parameters for the angle loop are the same for all results shown: $t_m^{r,a} = 1$ s, $t_o^{r,a} = 0.7$ s, $\zeta_m^a = \zeta_o^a = 0.999$, $\Delta^a = 1 - q^{-1}$. The inner moment loop was always designed without integral action, $\Delta^m = 1$, as integral action is included in the outer-loop design. The common design parameters for the inner loop are $\zeta_m^m = \zeta_o^m = 0.999$, $t_o^{r,m} = 0.15$ s. The risetime is varied between $t_m^{r,m} = 0.15$ s and $t_m^{r,m} = 0.2$ s.

In Figs. 16 and 17 the inner loop is neglected in the design of the outer loop. In this result, we investigated the effect of the speed of the inner loop on overall stability. The inner loop is designed to respond quickly for the results shown in Fig. 16, while a slower inner loop design was used in Fig. 17. The sensitivity functions corresponding to these two designs are plotted in Figs. 18 and 19, respectively.

In the next step, we investigated the effect of including the inner loop dynamics in the design plant for the outer loop, for both fast and slow inner loops. For the results shown in Figs. 20 and 21 the inner loop was used for the design of the outer loop, and a notch filter (eqns. 8 and 9) was included. Fig. 20 shows a design with a fast moment control loop, whereas the inner loop is slower for the results shown in Fig. 21. For these two cases the corresponding sensitivity functions are plotted in Figs. 22 and 23.

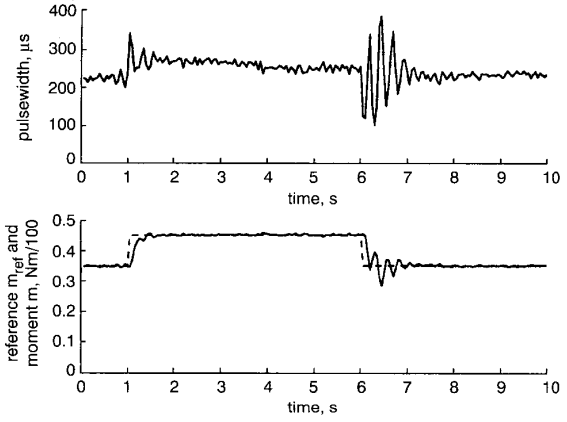

Fig. 12 *Muscle moment control with integral action. Design parameters (Section 3.1) are $t_m^r = 0.2$ s, $\zeta_m = 0.999$, $t_o^r = 0.15$ s, $\zeta_o = 0.999$*

– – – reference m_{ref}
—— moment m

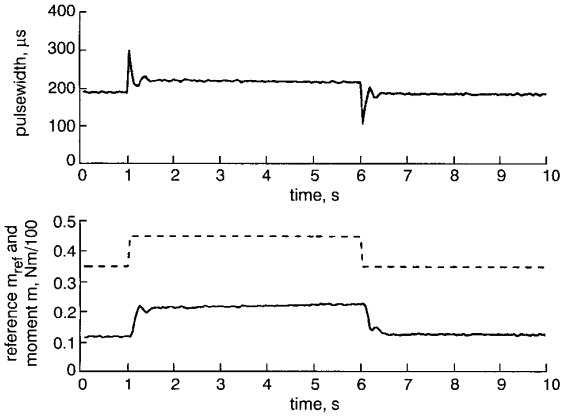

Fig. 13 *Muscle moment control without integral action. Design parameters as for Fig. 12*

– – – reference m_{ref}
—— moment m

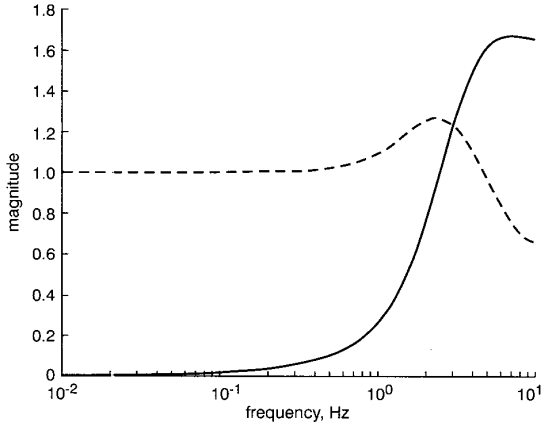

Fig. 14 *Bode magnitude plot of sensitivity $\tilde{S}$ and complementary sensitivity $\tilde{T}$ functions for moment controller in Fig. 12*

—— $\tilde{S}$
– – – $\tilde{T}$

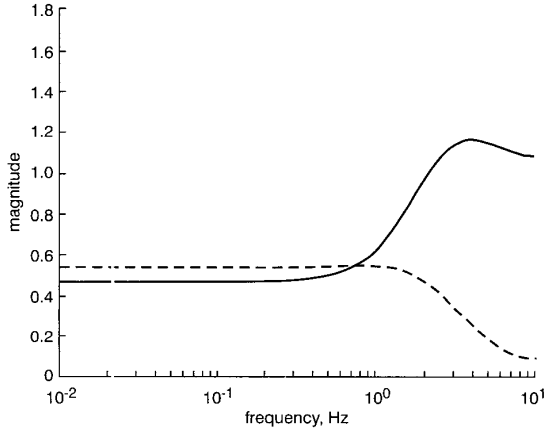

Fig. 15 *Bode magnitude plot of sensitivity $\tilde{S}$ and complementary sensitivity $\tilde{T}$ functions for moment controller in Fig. 13*

—— $\tilde{S}$
– – – $\tilde{T}$

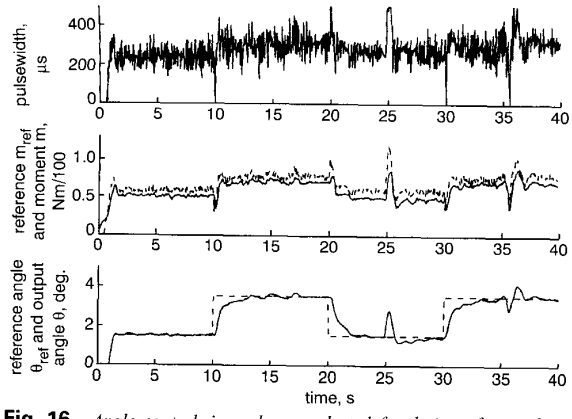

Fig. 16 *Angle control, inner loop neglected for design of outer loop. Fast inner loop ($t_m^{r,m} = 0.15$ s). Upper plot shows stimulation pulsewidth, middle plot shows moment reference and measured moment, and lower plot shows reference angle and measured angle*

--- reference
—— measured

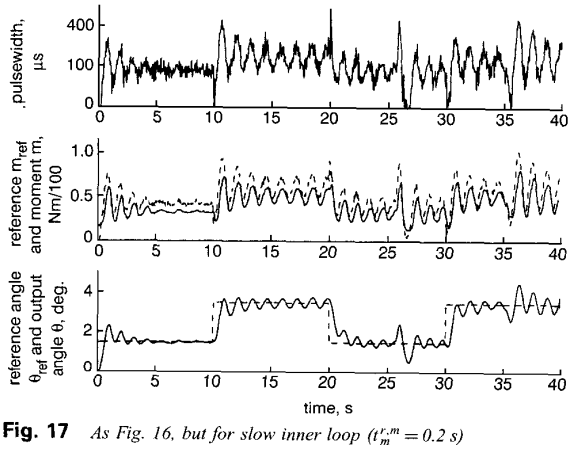

Fig. 17 *As Fig. 16, but for slow inner loop ($t_m^{r,m} = 0.2$ s)*

--- reference
—— measured

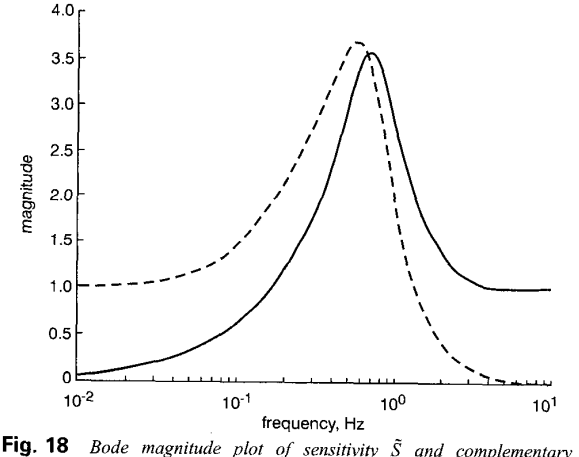

Fig. 18 *Bode magnitude plot of sensitivity $\tilde{S}$ and complementary sensitivity $\tilde{T}$ functions for angle controller used in Fig. 14. Inner loop neglected in angle controller design, but included in computation of $\tilde{S}$ and $\tilde{T}$*

—— $\tilde{S}$
--- $\tilde{T}$

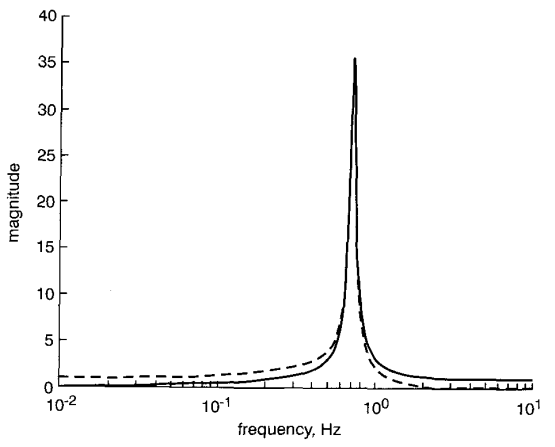

Fig. 19 *As Fig. 18, but for angle controller used in Fig. 17*

—— $\tilde{S}$
--- $\tilde{T}$

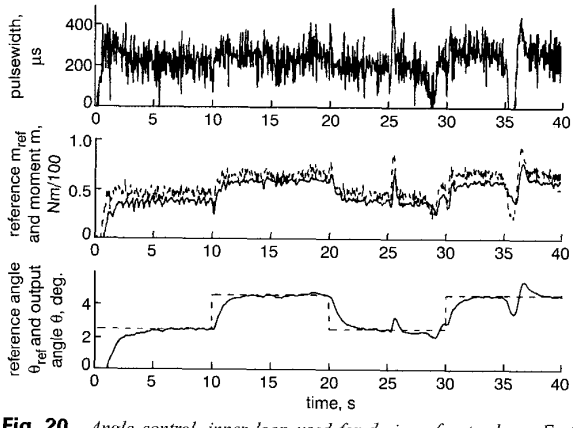

Fig. 20 *Angle control, inner loop used for design of outer loop. Fast inner loop ($t_m^{r,m} = 0.15$ s)*

--- reference
—— measured

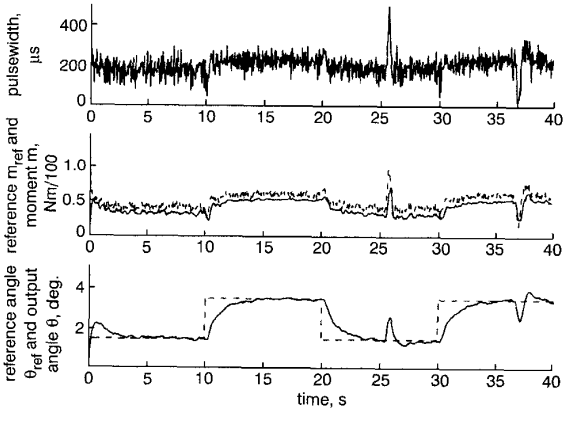

Fig. 21 *As Fig. 20, but for slow inner loop ($t_m^{r,m} = 0.2$ s)*

--- reference
—— measured

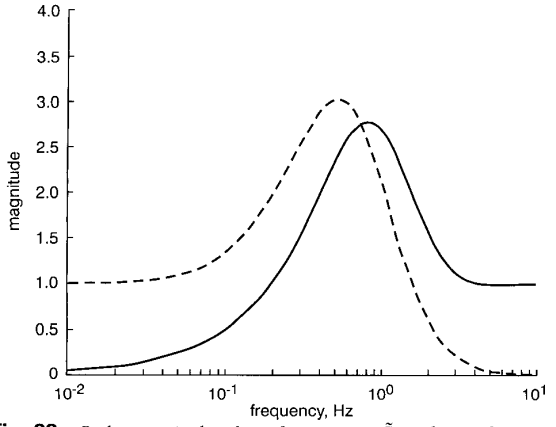

Fig. 22 *Bode magnitude plot of sensitivity $\tilde{S}$ and complementary sensitivity $\tilde{T}$ functions for angle controller used in Fig. 20. Inner loop used in angle controller design, and also included in computation of $\tilde{S}$ and $\tilde{T}$*

—— $\tilde{S}$
– – – $\tilde{T}$

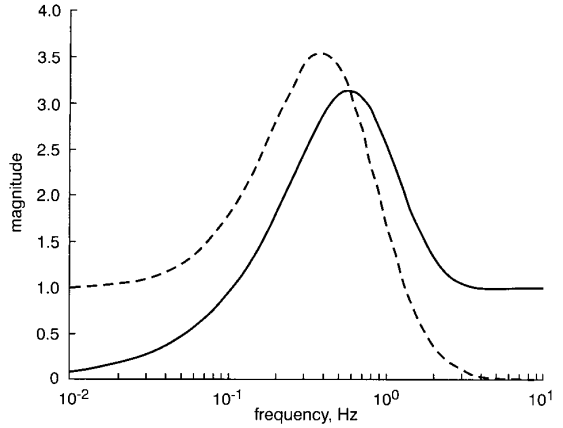

Fig. 23 *As Fig. 22, but for angle controller used in Fig. 21*

—— $\tilde{S}$
– – – $\tilde{T}$

Experiments were also carried out using a controller where the inner loop was used for the design of the outer loop but a notch filter was not included. Stable standing could not be achieved with this approach and results are therefore not shown. Reasons for this failure are discussed in Section 5.

5 Discussion of results

5.1 Ankle moment control results

The results shown in Figs. 12 and 13 suggest that if integral action is included in the moment loop controller, the closed loop tends to oscillate for a design with small risetime. An equivalent design without integral action remains stable and well damped. This observation is supported by the shape of the corresponding closed loop sensitivity functions $\tilde{S}$ complementary sensitivity functions $\tilde{T}$ (eqn. 7) which are shown in Figs. 14 and 15. The larger peak of the sensitivity functions of the controller with integral action (Fig. 12) explains the oscillations which are present in the closed loop responses. The oscillations have a frequency of approximately 4 Hz, which is seen to lie between the peak frequencies of the sensitivity functions. Thus, a higher bandwidth can be safely achieved using a controller without integral action. The fact that such a design results in a steady state error (Fig. 13) is of little importance for the cascaded control structure used here, as the steady state angle tracking can be accounted for by including integral action in the outer loop controller.

5.2 Body angle control results

In the first results presented in Section 4.4, the inner control loop was neglected for the design of the outer loop (see Figs. 16 and 17). This works well if the inner loop is fast enough (Fig. 16). For a slower inner loop this design leads quickly to problems as the delay introduced by the slow inner-loop response destabilises the outer loop (Fig. 17). An analysis of the corresponding closed loop sensitivity functions $\tilde{S}$ and complementary sensitivity functions $\tilde{T}$, which are shown in Figs. 18 and 19, verifies this observation.

Note that the nominal dynamics of the inner closed-loop system, neglected in the angle controller design, have been incorporated in the $\tilde{S}$ and $\tilde{T}$ plots for the angle control loop.

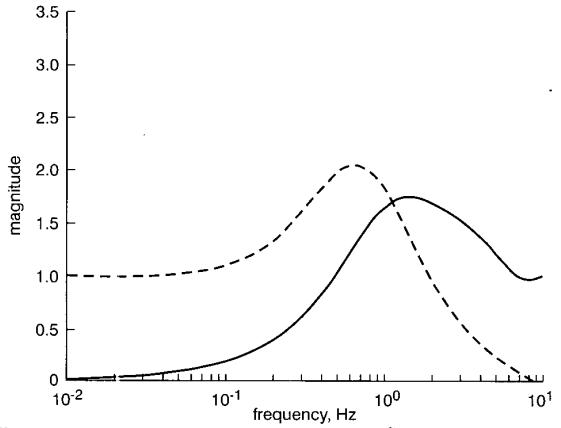

Fig. 24 *Bode magnitude plot of sensitivity $\tilde{S}$ and complementary sensitivity $\tilde{T}$ functions for angle controller designed without notch filter (Fig. 22). Inner loop used in angle controller design, and also included in computation of $\tilde{S}$ and $\tilde{T}$*

—— $\tilde{S}$
– – – $\tilde{T}$

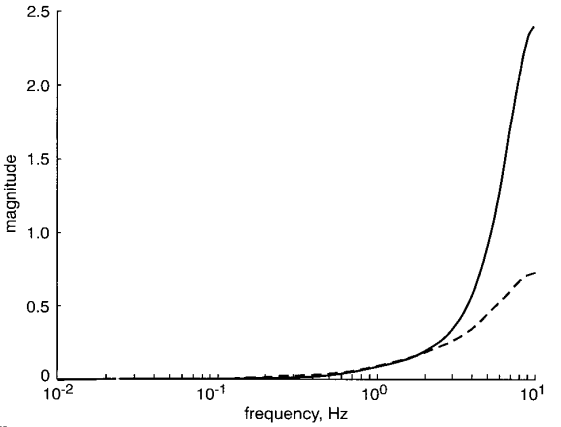

Fig. 25 *Bode magnitude plot of input sensitivity functions for angle controller designs with and without notch filter*

– – – with notch filter
—— without notch filter

The peak in the frequency responses of the design with slow inner loop at 0.72 Hz, Fig. 19, corresponds to a period of 1.4 s. This is equivalent to the period of the oscillation, which can be observed in the closed-loop time response shown in Fig. 17.

The dependence of the performance of the outer control loop on the inner loop can be reduced by accounting for the inner loop during the outer loop design; the inner loop dynamics are included in the design plant for the outer loop (see Section 3.3). In the time-response plots shown in Figs. 20 and 21, almost no difference can be observed in the output angle signal for the fast and slow inner loop designs. Comparing the corresponding Bode plots shown in Figs. 22 and 23, the peaks of the sensitivity and complementary sensitivity functions are not significantly different for the two designs. Moreover, the advantages of including the inner loop in the design are seen clearly when comparing the sensitivity plots in Figs. 19 and 23 for the slow inner loop. Thus, accounting for the inner loop during the outer-loop design significantly enhances the performance of the controller when the inner loop becomes slower.

The results discussed above where the inner loop is used for the outer loop design were achieved by including a notch filter in the controller design. As mentioned in Section 4, a similar design without the notch filter turned out to be unstable in the experiments. An explanation for this can be found by comparing the Bode plots of the sensitivity and complimentary sensitivity functions for a design without notch filter, which are shown in Fig. 24, with the corresponding design with notch filter (Fig. 22). One effect of the notch filter is that it causes the complementary sensitivity function T to decrease faster for high frequency, thus increasing robustness of the closed loop against measurement noise. The main effect, though, is seen in the input sensitivity functions for the two designs. The input sensitivity is defined as the transfer-function from measurement noise n to control signal u (see Fig. 8). These functions are plotted for the designs with and without notch filter in Fig. 25. Clearly, the design without notch filter is very much more sensitive to measurement noise. Indeed, simulations show that the controllers perform equally well without measurement noise, but that the controller without the notch filter becomes unstable as soon as noise is added. Since measurement noise is always present during the experiments, this explains the need to use a controller design with notch filter.

6 Conclusions

The experimental results show that the control system for unsupported standing performs reliably, and according to the design formulation. There are a number of design choices, appropriate to different situations, and the practical effect of each is clear. This allows easy 'tuning' during an experimental session. This is important since the complete design procedure, from muscle dynamics identification to control design, has to be carried out as quickly as possible while the subject is standing in the apparatus.

It is clear from theoretical considerations and from practical experience that having a slow inner loop for muscle moment control can have a destabilising effect on the overall closed-loop system. In general, it is important to maintain as high a bandwidth as possible for the inner loop, and this is best achieved when the inner loop is designed without integral action.

The ability to directly include the nominal inner loop dynamics as part of the design plant for the angle controller is advantageous, since stability can be maintained for slower inner loops.

It was seen that the notch filter design approach was required in this case. These results have important implications for experiments with paraplegic subjects, since with paralysed persons the inner loop can become slow due to fatigue and low muscle power. With a simple periodic test of muscle fatigue, and controller redesign, there is potential for maintenance of stability for a longer time.

The new moment control structure presented here has only one total ankle moment and a common stimulation pulsewidth for both legs (whereas we previously used separate left/right moment controllers [5]). We believe this is a better way to deal with left/right asymmetry in muscle power and fatigue rates (which is typical in paraplegics). Moreover, the moment control loop in this case is SISO, which makes design and implementation significantly simpler. With this approach we need only identify a single plant at each operating point, which is advantageous when working with impaired individuals since the identification process will take only half as long. However, it remains to be seen in paraplegic experiments whether this control strategy results in significant movement out of the sagittal plane.

In summary, the experimental results suggest that the preferred design choices for control of unsupported standing are:

(i) The inner loop should be as fast as possible, and should not include integral action.
(ii) The inner loop dynamics should be incorporated as part of the design plant for the angle controller.
(iii) The notch filter approach should be used in the angle controller synthesis.

The next step in our research is to verify the modified control system for unsupported standing in experiments with paraplegic subjects.

7 References

1 BENTON, L.A., BAKER, L.L., BOWMAN, B.R., and WATERS, R.L.: 'Functional electrical stimulation – a practical clinical guide'. 1981, Technical report, Rancho Los Amigos Rehabilitation Engineering Center, Downey, California
2 KRALJ, A., and BAJD, T.: 'Functional electrical stimulation: Walking and standing after spinal cord injury' (CRC Press, Florida, 1989)
3 DONALDSON, N., and YU, C.-H.: 'FES standing: Control by handle reactions of leg muscle stimulation (CHRELMS)', *IEEE Trans. Rehabil. Eng.*, 1996, **4**, pp. 280–284
4 DONALDSON, N., and YU, C.-H.: 'A strategy used by paraplegics to stand up using FES', *IEEE Trans. Rehabil. Eng.*, 1998, **6**, pp. 162–167
5 HUNT, K.J., MUNIH, M., and DONALDSON, N.: 'Feedback control of unsupported standing in paraplegia. Part I: optimal control approach', *IEEE Trans. Rehabil. Eng.*, 1997, **5**, pp. 331–340
6 MUNIH, M., DONALDSON, N., HUNT, K.J., and BARR, F.M.D.: 'Feedback control of unsupported standing in paraplegia. Part II: experimental results', *IEEE Trans. Rehabil. Eng.*, 1997, **5**, pp. 341–352
7 GRAUPE, D., and KOHN, K.H.: 'Functional electrical stimulation for ambulation by paraplegics' (Krieger Publishing Company, Florida, USA, 1994)
8 PETROFSKY, J.S., HEATON, H.H., and PHILLIPS, C.A.: 'Outdoor bicyle for exercise in paraplegics', *J. Biomed. Eng.*, 1983, **5**, pp. 292–296
9 PONS, D.J., VAUGHAN, C.L., and JAROS, G.G.: 'Cycling device powered by the electrically stimulated muscles of paraplegics', *Med. Biol. Eng. Comput.*, 1989, **27**, pp. 1–7
10 DONALDSON, N.: 'Practical ankle controllers for unsupported standing in paraplegia'. Proceedings of Ljubljana FES Conference, 1993, pp. 61–64
11 DONALDSON, N., BARR, F.M.D., PHILLIPS, G.F., and PERKINS, T.A.: 'Unsupported standing of paraplegics by stimulation of the plantarflexors: some results from the wobbler apparatus', *in* PEDOTTI, A., FERRARIN, J., and RIENER, R. (Eds.): 'Neuroprosthetics: from basic research to clinical application' (Springer-Verlag, 1996)

12 HUNT, K.J., MUNIH, M., DONALDSON, N., and BARR, F.M.D.: 'Optimal control of ankle joint moment: toward unsupported standing in paraplegia', *IEEE Trans. Autom. Control*, 1998, **43**, pp. 819–832
13 DONALDSON, N., MUNIH, M., PHILLIPS, G.F., and PERKINS, T.A.: 'Apparatus and methods for studying artificial feedback-control of the plantarflexors in paraplegics without interference from the brain', *Med. Eng. Phys.*, 1997, **19**, (6), pp. 525–535
14 PHILLIPS, G.F., ADLER, J.R., and TAYLOR, S.J.G.: 'A portable programmable eight-channel surface stimulator'. Proceedings of Ljubljana FES Conference, 1993, pp. 166–168
15 LJUNG, L.: 'System identification: Theory for the user' (Prentice Hall, 1999, 2nd edn.)
16 HUNT, K.J., MUNIH, M., DONALDSON, N., and BARR, F.M.D.: 'Investigation of the Hammerstein hypothesis in the modelling of electrically stimulated muscle', *IEEE Trans. Biomed. Eng.*, 1998, **45**, pp. 998–1009
17 HUNT, K.J.: 'Stochastic optimal control theory with application in self-tuning control' vol. 117 of 'Lecture notes in control and information sciences' (Springer-Verlag, Berlin, 1989)
18 Åström, K.J., and Wittenmark, B.: 'Computer controlled systems' (Prentice Hall, 1997, 3rd edn.)
19 Kučera, V.: 'Discrete linear control: the polynomial equation approach' (Wiley, Chichester, 1979)
20 http://www.mech.gla.ac.uk/~tschauer/wobbler.htm